Deformation Behavior of Cadmium Telluride Stressed at Elevated Temperatures

J. Shen, R. Balasubramanian, D.K. Aidun, L.L. Regel, and W.R. Wilcox

(Submitted 8 August 1994; in revised form 30 October 1997)

CdTe crystals were uniaxially compressed along several crystallographic axes at temperatures from 773 to 1353 K. The applied stress ranged from 14 to 74% of the critical resolved shear stress (CRSS) measured in the authors' laboratory. The deformed specimens were annealed without applying stress at temperatures from 573 to 1073 K. No twins were observed after the above operations. Dense slip bands were observed on most of the compressed specimens. Secondary slip systems were activated in some experiments. CdTe crystals were sheared along {111}<112> at 1073 K with a load of 40% CRSS. Slip bands, but no twins, were observed. Synchrotron x-ray topography was used to study in situ the effect of stress on crystal deformation. CdTe specimens were uniaxially stressed in tension along <112> at 293 to 673 K. When the load reached ~50% of the CRSS, the topograph began to distort, indicating the beginning of plastic deformation. No twins were observed on the stressed specimens.

Keywords cadmium telluride, critical resolved sheer stress, crystal growth, deformation, dislocations, solidification, twinning

1. Introduction

Twins are common defects in CdTe and CdZnTe grown by most techniques (Ref 1). Device performance is severely degraded by the presence of twins (Ref 2, 3). Only 180° rotation twins have been observed in zinc-blend structures (Ref 4-7). Twins in CdTe and its alloys commonly appear in two morphologies. One is a lamellar twin that penetrates through the whole grain with two parallel twin boundaries. The other is a lateral twin that terminates inside a grain with stepped or straight boundaries (Ref 4, 8).

J. Shen, R. Balasubramanian, D.K. Aidun, L.L. Regel, and **W.R. Wilcox,** International Center for Gravity Materials Science and Applications, Clarkson University, Potsdam, NY.

In classical mechanical metallurgy, it is believed that twinning deformation of the face-centered cubic (fcc) structure might occur only within some low temperature range and at a high strain rate (Ref 9). Twinning in the fcc structure is thought possible only when slip systems are restricted (Ref 9). On the other hand, annealing twins usually form when a plastically deformed crystal is annealed at elevated temperatures. Annealing twins are generally broader with straighter boundaries than mechanical twins; most fcc metals form annealing twins (Ref 9). Deformation and annealing twins were reported in gold-silver alloys and copper, which have the fcc structure (Ref 9-11). Previous reports claimed or speculated on the appearance of deformation twins in Si, Ge, InSb, GaSb (Ref 12), and CdTe (Ref 13-15).

To measure the critical resolved shear stress (CRSS) and observe dislocations, CdTe and CdZnTe have been deformed along several axes at temperatures from 293 to 1136 K at various strain rates (Ref 16, 17-19). It was not mentioned in these works if new twins were observed. Slip lines were observed on

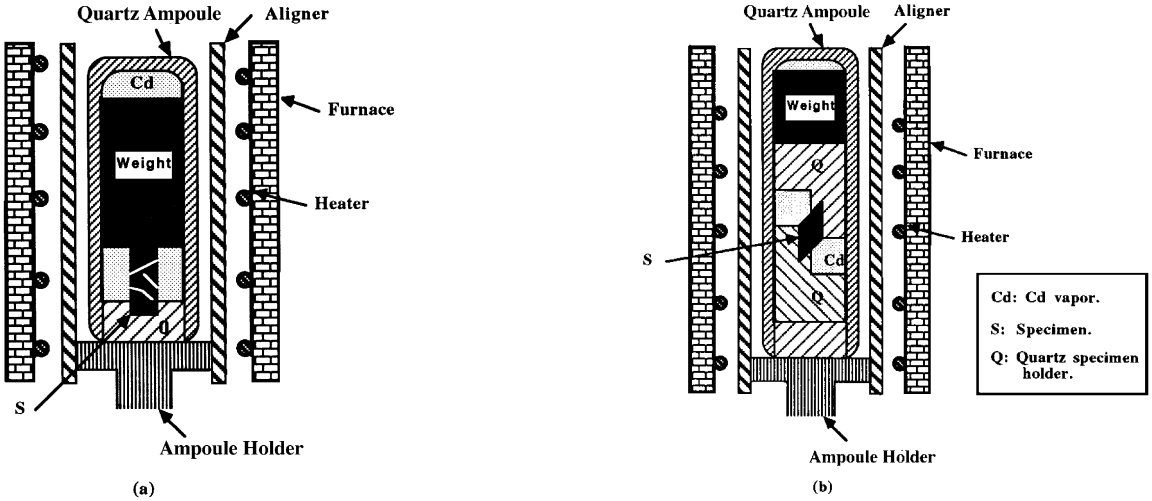

Fig. 1 Schematics of compression and shear devices. (a) For compression experiments. (b) For shear experiments. The furnace diameter is approximately 35 cm; the length is approximately 100 cm.

the deformed CdTe (Ref 16, 19). To investigate the origin of twins, Vere et al. (Ref 1) compressed CdTe at 298 to 598 K at a strain rate of 2.3×10^{-4}/s to 2.3×10^{-3}/s. No new twins were observed in specimens compressed to strains of 3 to 5% before fracture (Ref 1). Slip deformation was reported. Owing to evaporation, the test temperature used by Vere et al. did not exceed 598 K.

Because of the controversies and experimental difficulties mentioned above, a series of deformation tests were conducted for CdTe at temperatures up to about 0.99 of the melting point. The effort of this work concentrated on the observation of deformation twins and the deformation behavior of CdTe at elevated temperatures.

2. Experiments

Uniaxial compression, shearing, and uniaxial tensile experiments were conducted on CdTe specimens along several loading axes. The experimental details are as follows.

2.1 Compression and Shear

Devices for uniaxial compression and shearing are illustrated in Fig. 1. Weights rested on top of the specimen to maintain constant stress within the specimen. Loads were selected to generate a stress along the active slip systems at a magnitude of 14 to 74% of the CRSS at each corresponding test temperature. The relationship of CRSS versus temperature shown in Fig. 2 was measured previously (Ref 17). An equation fit to the data in Fig. 2 was used to calculate the loads. The stress calculation is as follows:

- Fitting equation:

$$\text{CRSS} = 12.25\exp(-0.00279T) \quad \text{(MPa)}$$

- $\sigma = W/A$ where σ is the normal stress (in MPa) along the loading axis; W is the force from the applied weight (in N); and A is the cross section of the specimen (in m^2).
- The resolved shear stress along a potential slip system is $\sigma_{rs} = \sigma S$ where S is the Schmid factor of the slip system.
- The ratio of applied stress along slip system to the CRSS is $R = \sigma_{rs}/\text{CRSS}$.

Based on the above calculation, the normal stress and percentage of CRSS for all experiments were obtained and listed in Table 1.

Specimens for compression tests were compressed at elevated temperatures for 30 min to 20 h, respectively. The engineering strain of specimens was calculated using $(L_0 - L)/L_0$, where L_0 is the original specimen length and L is the length after compression. Dividing the engineering strain by the compression time yielded an estimated average strain rate of approximately 1.7×10^{-5}/s to 9.2×10^{-8}/s. Specimens for shear experiments were sheared at 800 °C for 0.5 h. The experimental parameters are listed in Table 1. The strain rate in the

Table 1 Summary of deformation experiments

Code	Size, mm	Plane	Load axis	σ, MPa	CRSS, %	Temperature, K	Time, h	Strain rate, 10^{-5}/s	Strain, %	Active slip system	EPD, 10^5/cm^2 Before	EPD, 10^5/cm^2 After
Test-P1A11	13.8 × 5.3 × 1.78	(511)	[11$\bar{6}$]	0.47	45	1173	10	…	0	None	…	…
Test-P1A12	13.8 × 5.3 × 1.78	(11$\bar{1}$)	[112]	0.47	41	1173	10	…	0	one	3.11	2.12
Test-P1A13	7.3 × 5.3 × 1.78	(511)	[11$\bar{6}$]	0.3	44	1323	10	…	Failed	…	…	…
Test-P1A21	13.8 × 5 × 1.85	(11$\bar{1}$)	[112]	0.55	16-64	773-1273	0.5	…	…	(1$\bar{1}$1)[$\bar{1}$0$\bar{1}$] (1$\bar{1}$1)[0$\bar{1}$1]	2.25	…
Test-P1A22	13.8 × 5 × 1.85	(511)	[11$\bar{6}$]	0.55	18-71	773-1273	0.5	…	…	(1$\bar{1}$1)[0$\bar{1}$0] (1$\bar{1}$1)[10$\bar{1}$]	…	…
Test-P1A23	…	(11$\bar{1}$)	[112]	0.55	74	1323	0.5	…	Failed	…	…	…
T1-P1A11	16.5 × 4.95 × 2.45	(11$\bar{1}$)	[123]	0.42	14-42	773-1173	5-10	…	0	None	3.89	3.89
T1-P1A12	16.5 × 4.95 × 2.45	(11$\bar{1}$)	[123]	0.42	56	1273	0.5	1.7	3.1	(111)[$\bar{1}$01] Secondary (1$\bar{1}$1)[101]	~3.89	~3.5-4.67
T1-P1A13	16.5 × 4.95 × 2.45	(301)	[010]	0.42	49	1273	0.5	1.7	3.1	(111)[0$\bar{1}$1] ($\bar{1}$1$\bar{1}$)[0$\bar{1}$1]	…	…
T1-P1A14	16 × 5.02 × 2.49	(111)	…	0	0	573-1073	5	…	0	None	~3.5	2.96
T1-P1A15	16 × 5.02 × 2.49	(11$\bar{1}$)	[123]	0.18	27	1323	1	…	0	None	2.96	9.53
T2-A1	15.2 × 4.23 × 1.4	($\bar{1}$11)	[110]	0.36	47	1323	20	9.2×10^{-3}	0.66	(111)[0$\bar{1}$1] ($\bar{1}$11)[0$\bar{1}$1]	1.8	>100
T2-A21	15.2 × 4.3 × 1.34	($\bar{1}$11)	[110]	0.36	50	1323	10	…	…	(111)[0$\bar{1}$1] ($\bar{1}$11)[0$\bar{1}$1]	…	…
T2-A22	…	($\bar{1}$11)	[110]	0.37	55	1353	0.5	…	Failed	…	…	…
T3-A1	14.8 × 4.49 × 2.13	($\bar{1}$10)	[115]	0.23	36	1353	0.5	7.7	>13.9	($\bar{1}$11)[101] ($\bar{1}$1$\bar{1}$)[0$\bar{1}$1]	…	…
T3-A2	14.9 × 4.1 × 2.12	($\bar{1}$10)	[115]	0.28	44	1346	20	…	Failed	…	…	…
Syn (tensile)	12.5 × 8 × 0.36	($\bar{1}$11)	[1$\bar{1}$2]	2.3	50	293-673	…	…	…	…	…	…
T4-2 (shear)	15.6 × 10.6 × 1.89	($\bar{1}$10)	($\bar{1}\bar{1}$1)[112]	τ = 0.28 ($\bar{1}\bar{1}$1) [112]	40	1073	0.5	…	…	(1$\bar{1}$1)[$\bar{1}$0$\bar{1}$] ($\bar{1}$11)[$\bar{1}$0$\bar{1}$] (111)[01$\bar{1}$]-Secondary	…	…

shear experiments could not be estimated due to the difficulty in strain measurement.

CdTe specimens were mined from ingots grown by the vertical Bridgman technique. The starting materials were 6*N* purity provided by II-VI, Inc., Saxonburg, PA. The growth parameters are described in Ref 20. The x-ray Laue method was used to orient the crystals. The specimens were cut by a wire saw, then mechanically polished with alumina particles of 5.0, 0.3, and 0.05 μm. The specimens were finally polished in a 2% Br_2-methanol solution for 4 min.

The specimens were observed under optical microscopy to record their surface features before putting them in ampoules. Etch pit density (EPD) and specimen dimensions were measured before deformation experiments. The EPD was an average from counts on five randomly selected areas. The data for each specimen are summarized in Table 1. The EPD was compared only on {111} planes by a Nakagawa etchant, which is relatively reliable for CdTe. For an experiment, a specimen held by a quartz plug was put in a well-cleaned ampoule with elemental Cd shot to prevent the evaporation of Cd and Te from the specimen surfaces. For a specimen stressed above 973 K, quartz weights were placed on top of the specimen. Weights made of Ni-Cr alloy were used to establish sufficient stress in specimens stressed at temperatures below 973 K. The ampoule was evacuated to 10^{-6} Torr and sealed by a torch. Then the ampoule was put in a vertical furnace and heated following the parameters listed in Table 1. After deformation, the EPD and specimen dimensions were measured again. The surfaces of the stressed specimens were examined under optical microscopy and scanning electron microscopy (SEM). To distinguish the slip bands from twin lamellae, x-ray Laue patterns and SEM with electron channeling patterns (SEM/ECP) were used.

Some previously deformed specimens were annealed without load. The deformed specimens were cleaned in 2% Br_2-methanol and sealed in an ampoule evacuated to 10^{-6} Torr. Cadmium shot was put in the ampoule to prevent evaporation. The annealing parameters are listed in Table 1. After isothermal annealing, the specimens were cooled to room temperature at a rate of approximately 50 to 100 °C/h. Again, etching, x-ray Laue patterns, and SEM/ECP were used to characterize the annealed specimens.

Table 2 Parameters of the beamline X23-A

Energy spectrum available	5-30 KeV
Equivalent wavelength	~2.5-0.4 Å
Photon flux for diffraction	10^4 photons/mm^2 · s
Bandpass ($\Delta\lambda/\lambda$)	1%
Crystal type	Si (111) or Si (220)

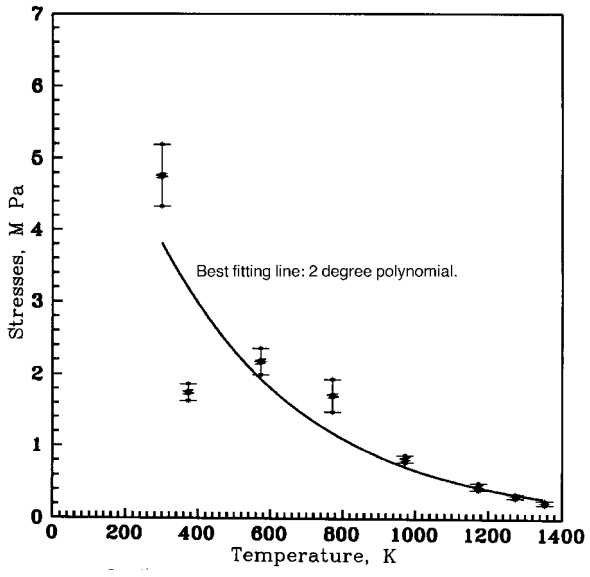

Fig. 2 Critical resolved shear stress of CdTe versus temperature (Ref 17)

2.2 Tensile

For the tensile experiments, synchrotron x-ray topography was used to observe in situ the deformation behavior of CdTe at 293 to 693 K. Rectangular CdTe specimens with dimensions of $13 \times 8 \times 0.6$ mm were mounted on glass microscope slides with a thermoplastic adhesive, then shaped as dogbones by grinding the centers of the long side edges with a 200-grit silicon carbide grinding wheel. The specimens were ready for tensile tests after a final chemical polishing with 2% Br_2 in methanol. The final dimensions of the tensile specimens are shown in Table 1. The in situ synchrotron x-ray imaging was carried out using the NIST Material Science Beamline X-23A3 at the National Synchrotron Light Source at Brookhaven, New York. The parameters of the apparatus are listed in Table 2, and the experimental setup is shown in Fig. 3 (Ref 21).

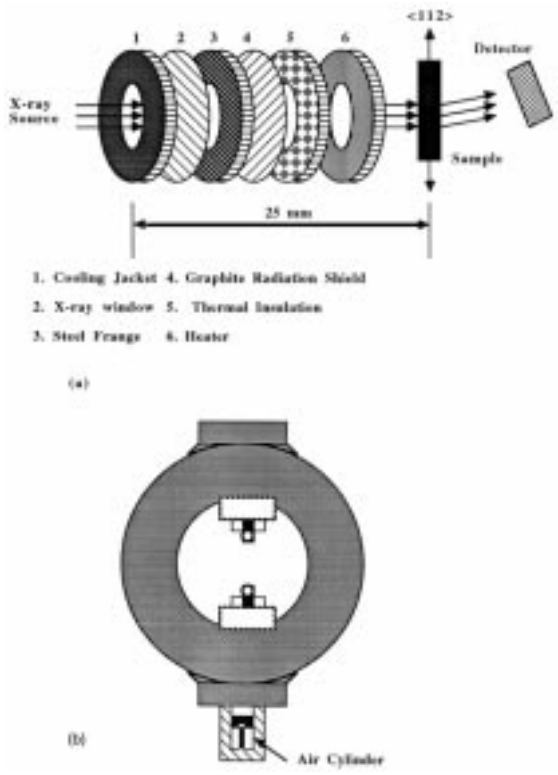

Fig. 3 Experimental setup for in situ observation during tensile experiments by synchrotron x-ray topography. (a) Setup. (b) Load cell

A constant load was applied and controlled by an air cylinder connected to the load cell. A constant strain rate tensile test could not be performed because the load was controlled only by a pressure regulator, and the loading had to be stopped periodically to record the topographic images. The corresponding data for tensile experiments are listed in Table 1. A white x-ray beam was selected as the radiation source for transmission diffraction topography. Topographic images were detected by a charge coupled device (CCD) camera and recorded on a videorecorder and on high-resolution x-ray film.

3. Results and Discussions

3.1 Structure of Twins in CdTe

To determine the structural types of twins in CdTe, the etching feature of a {111} twin was compared with its host matrix.

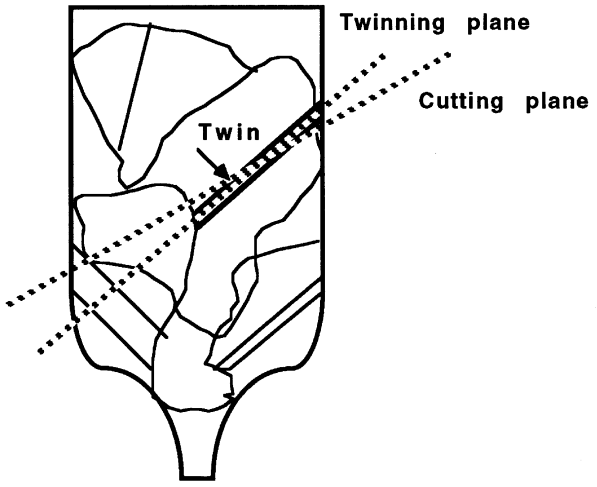

Fig. 4 Cut across a twin in CdTe at an interception angle of approximately 3°

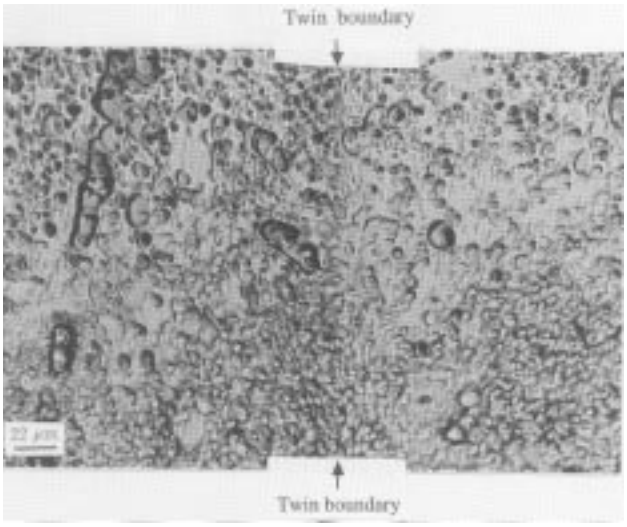

Fig. 5 Morphology of etch pits across a twin boundary on a (111)A plane of CdTe. Nakagawa etchant, 40 s

Nakagawa etchant that reveals etch pits only on {111}A surfaces was used in this work. If a CdTe grain was cut as shown in Fig. 4, etch pits would be revealed by the Nakagawa etchant only on one side of an inversion twin boundary, because both (111)A and B would be exposed by cutting across an inversion twin boundary. If it is a rotation twin, etch pits would be revealed on both sides of the twin boundary on {111}A surfaces. Furthermore, the shape of the etch pits on one side of the boundary would be mirror symmetric to that on the other side, because a (111)A orientation would not be changed in both the twin and its host matrix by a rotation operation. The mirror-symmetric etch pit pattern can be explained by the fact that the structure of a rotation twin can be obtained by rotating a portion of the matrix around its <111> axis by either 60° or 180° with respect to the host matrix (60° and 180° rotations give the same twin structure for zinc-blend structure because the lattice is threefold symmetric around <111> axes). A 180° rotation results in the mirror symmetry between the twin and its host matrix lattices. Hence, the etch pit pattern is also mirror symmetric.

As shown in Fig. 5, the etch pits appeared on both sides of a twin boundary. The surface was prepared with the method described in the above paragraph. The shapes of the etch pits on each side were roughly mirror symmetric to the twin boundary that is shown by the arrows in Fig. 5. No perfect mirror-symmetric etch pits were observed because the cutting line was about 3° off the {111} twinning plane to expose both the twin and the host matrix. Based on the reasons explained in the preceding paragraph, it can be concluded that the twins in CdTe are 180° rotation twins. Unlike inversion twins, it cannot be determined whether the rotation twins in CdTe were induced at the growth interface or by mechanical deformation. Thus, another method had to be considered to investigate the origin of twinning.

3.2 Compression Deformation

As shown in Table 1, specimens were uniaxially compressed along (11$\bar{6}$), [112], [123], [010], [110], or [115] at temperatures ranging from 773 to 1353 K. Crystals with the fcc structure have the {111}<110> dislocation slip systems and {111}<112> twinning systems (Ref 9), assuming that twinning deformation occurs by shear stress along <112>. Among the loading axes, [010] and [110] should be the favored orientations for twinning deformation (if twins are caused by mechanical deformation), because the ratio of slip Schmid factor to twinning Schmid factor is the lowest for these axes, as shown in Table 3. Loading along an axis with a twinning Schmid factor larger than a slip Schmid factor, a higher fraction of the total load would be applied to the twinning systems than to the slip systems.

No new twins were observed on specimens stressed along those favorite axes nor any other axes at a temperature up to 1353 K and with a stress up to 71% of CRSS. Dense slip bands were observed on the plastically deformed specimens. In most cases, these slip bands covered the entire surface. In Table 1, the change in etch pit density was used to estimate the change in dislocation density that could have resulted from the presence of slip bands. Etch pit density is not shown in Table 1 for those specimens that either failed during compression or had

planes other than {111}. The Nakagawa etchant used in this work is reliable only on the {111} plane.

As an example, Fig. 6(a) shows two sets of slip bands on a specimen stressed along [010] at 1273 K for 30 min. Each group of slip bands in this figure was indexed by calculating the interception angle of an activated slip plane with the observed surface. As shown in Fig. 6(a) and (b), the calculated angles match the measured angles. Only two of the eight potential slip systems were activated by loading along [010]. As detailed in the next section, by comparing the x-ray Laue patterns and SEM electron channeling patterns, the slip bands in Fig. 6 were confirmed not to be twins. Neither twins nor slip bands could be seen on the specimens without plastic deformation.

In one case, a secondary slip system was activated after compression along [123] at 1273 K with 56% of CRSS and a nominal strain of only 3.1%. Activation of the secondary slip system in CdTe compressed along <123> at room temperature was also reported by Orlova and Sieber using transmission electron microscopy (Ref 19). Their specimen was plastically deformed to a strain of only 2.5%. Specimens with <123> loading axes are often used to measure the CRSS of CdTe, because the CRSS would result from only one slip system and hence deformation hardening could be avoided in the early deformation stage (Ref 16, 21). However, the above observations imply that the intersection slip could have occurred at an early deformation stage. Consequently, the actual CRSS may have been lower than what was reported.

A lateral twin that terminated in a grain did not propagate after compression at 1173 K for 10 h with a stress of 45% CRSS. Therefore, even if a twin might be caused by deformation, it seems unlikely that it would propagate during in situ annealing and cooling, at least at these stress levels.

The above observations suggest that stresses induced during a growth process would be released by deformation through dislocations gliding on slip planes, rather than by twinning deformation. CdTe has a high ionicity and a weak atomic bonding at elevated temperatures. Consequently, before triggering twinning, the crystal would deform through dislocations moving on slip planes. Furthermore, it was observed that long before the stress reached the engineering CRSS, dislocations began to move along slip directions at elevated temperatures (Ref 17).

In addition to temperature and load, strain rate is another factor that may influence deformation twinning in crystals. For fcc structures, a low temperature and a high strain rate are believed to favor twinning deformation (Ref 9). Although the strain rate in this work was very low (about 1.7×10^{-5}/s to 9.2×10^{-8}/s), these rates are closer to the strain rate in directional solidification than the rates applied in Vere's work. During direct solidification, the strain rate is likely to be very low because of a low temperature gradient, low translation rate, and a slow cooling rate. In Vere's work, slip but not twinning was observed on specimens compressed at 298 to 598 K with a strain rate ranging from 2.3×10^{-2}/s to 2.3×10^{-4}/s (Ref 1). From Vere's work and the present results, it appears that twins are not caused by stress during solidification. In directional solidification, a CdTe ingot experiences temperatures ranging from 1363 K to room temperature. This temperature range was almost completely covered in this work and in Vere's work. In the present study, the authors did not stress specimens at temperatures above 1353 K, with a load higher than 74% of CRSS, and annealing time longer than 20 h, because twinning seems unlikely to occur after dislocations start to move extensively.

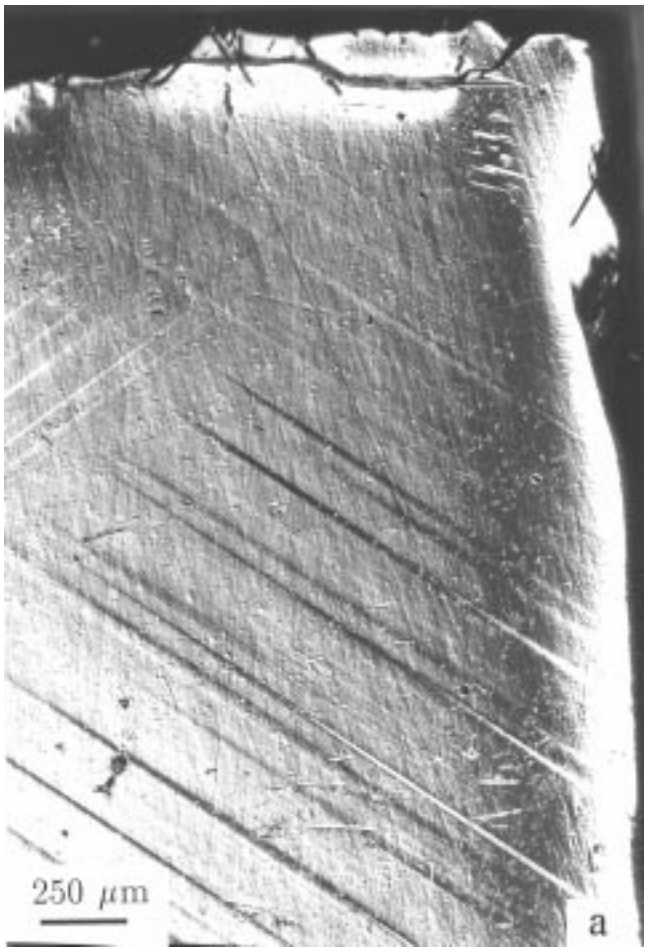

(b)

Fig. 6 (a) Two sets of slip bands on a (301) plane. The specimen was compressed along [010] at 1273 K for 30 min with a load of 49% CRSS, 3.1% strain. (b) Geometrical position of the slip bands

As shown in Table 1, no new twins were observed in a specimen deformed with 3.1% strain, then annealed free of load at 573 to 1073 K for 5 h. Also, as shown in Table 1, etch pit density (EPD) in specimens was increased by compression at temperatures higher than 1323 K. Figure 7 shows the difference in EPD of a specimen before and after compression at 1323 K. As shown in Fig. 7(b), dense etch pits covered the entire surface of the compressed specimen. The change in EPD caused by compression at temperature below 1323 K was not significant. Only in one case was the EPD at the corners of a specimen considerably increased by compression at 1273 K, as shown in Table 1. Two sets of slip bands were observed at the corners of the specimen. One set was from a primary slip system, and the other was from a secondary slip system. The increase in EPD at the corners can be attributed to local deformation caused by the uneven contact between the specimen and the applied weight. The strain at the corners could be greater than the average strain.

A well-defined alignment of etch pits along slip lines was infrequently observed on the deformed specimens, unlike in Si and InSb where alignment was clearly observed (Ref 12). In most cases, entire surfaces were covered by irresolvable etch pits. All of the above observations suggest that dislocations in the weakly bonded CdTe glide and multiply at temperatures close to its melting point more easily than in other crystals with diamond or zinc blend structures.

The appearance of slip bands and the occurrence of plastic deformation in the specimens compressed with a load lower than the CRSS was not anticipated before this study. This observation could have resulted from the difference in strain rate. A high strain rate would cause a higher apparent CRSS for some materials, because deformation mechanisms such as dislocation climbing and aging hardening are time dependent. As mentioned previously, the strain rate in this work was extremely low due to the experimental setup (as low as 10^{-8}/s). The strain rate used to measure the CRSS was relatively high (10^{-4}/s).

As listed in Table 1, some of the compression tests conducted at temperatures close to the melting point were not successful. In most cases, the specimens were sandwiched between the weight and the sample holder after being maintained at temperatures close to the melting point for periods longer than 10 h or with a load larger than 50% of CRSS. Plastic deformation was observed on a specimen that was heated to 1353 K then quenched. As illustrated in Fig. 8, a portion of the specimen material had flowed down from its top at 1353 K with 36% CRSS when the ampoule was cooled rapidly. The lower

Table 3 Slip and twinning systems

Loading axis	Active slip system (SS)	Maximum Schmid factor of SS (MSS)	Active twinning system (TS)	Maximum Schmid factor of TS (MTS)	Ratio of MSS/MTS
[11$\bar{6}$]	(1$\bar{1}\bar{1}$)[0$\bar{1}$1], (1$\bar{1}$1)[10$\bar{1}$]	0.4512	(1$\bar{1}\bar{1}$)[1$\bar{1}$2] (1$\bar{1}$1)[1$\bar{1}\bar{2}$]	0.4466	1.01
[112]	(1$\bar{1}\bar{1}$)[101], (1$\bar{1}$1)[0$\bar{1}\bar{1}$]	0.4082	(1$\bar{1}\bar{1}$)[$\bar{2}$11] (1$\bar{1}$1)[121]	0.3928	1.04
[123]	(1$\bar{1}\bar{1}$)[101]	0.4666	(1$\bar{1}\bar{1}$)[$\bar{2}$11]	0.4714	0.99
[010]	(111)[0$\bar{1}$1], (111)[$\bar{1}$10] (1$\bar{1}\bar{1}$)[0$\bar{1}\bar{1}$], (1$\bar{1}\bar{1}$)[110] (1$\bar{1}$1)[0$\bar{1}\bar{1}$], (1$\bar{1}$1)[[$\bar{1}\bar{1}$0] (11$\bar{1}$)[0$\bar{1}\bar{1}$], (11$\bar{1}$)[1$\bar{1}$0]	0.4082	(111)[1$\bar{2}$1] (1$\bar{1}\bar{1}$)[12$\bar{1}$] (1$\bar{1}$1)[121] (11$\bar{1}$)[1$\bar{2}$1]	0.4714	0.87
[110]	(111)[0$\bar{1}$1], (111)[$\bar{1}$01] (11$\bar{1}$)[0$\bar{1}\bar{1}$], (11$\bar{1}$)[1$\bar{1}$0]	0.4082	(111)[11$\bar{2}$] (11$\bar{1}$)[112]	0.4714	0.87
[115]	(1$\bar{1}\bar{1}$)[101], (1$\bar{1}$1)[0$\bar{1}\bar{1}$]	0.4536	(111)[11$\bar{2}$]	0.4889	0.93
($\bar{1}\bar{1}$1)[112] shear plane	($\bar{1}\bar{1}$1)[$\bar{1}$0$\bar{1}$] (shear) ($\bar{1}$11)[$\bar{1}$0$\bar{1}$], (1$\bar{1}$1)[0$\bar{1}\bar{1}$]	0.4082	($\bar{1}\bar{1}$1)[112]	1.0	0.4082

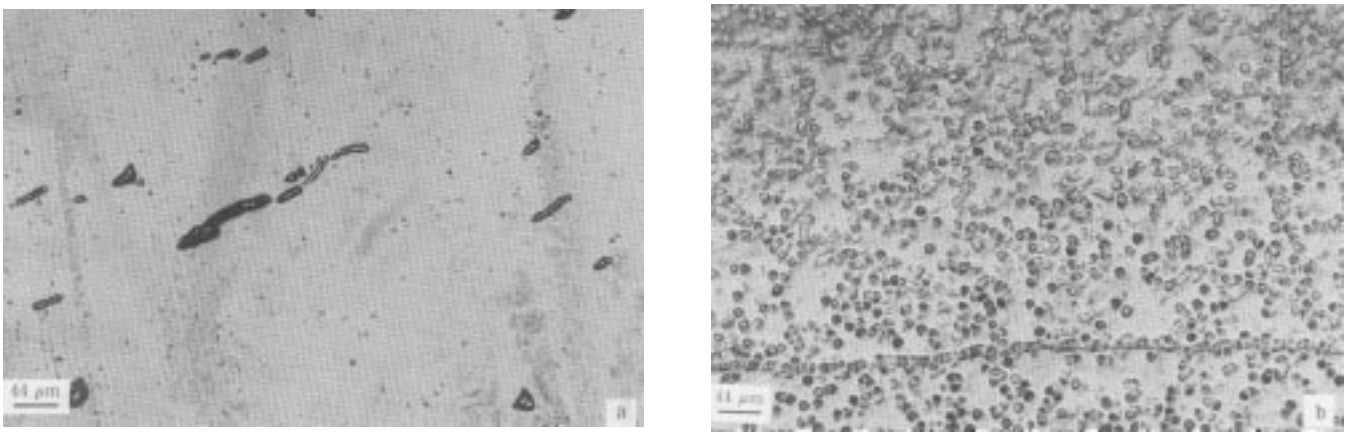

Fig. 7 Etch pit patterns on a (1$\bar{1}\bar{1}$)A CdTe before and after compression along [110] at 1323 K with 47% CRSS for 20 h, 0.66% strain. Nakagawa etchant, 40 s. (a) Before compressions, EPD is $1.85 \times 10^5/cm^2$. (b) After compression, EPD is $>10^7/cm^2$.

part of the specimen still maintained its original shape, but with dense slip bands on its surfaces. Thus, the plastic flow might be due either to severe slip or creep deformation that occurred before the quenching process.

3.3 Shearing Deformation

The shear specimens were designed with a $(\bar{1}11)$ shear plane and a [112] shear direction. The shear stress was 40% of the CRSS along the $(\bar{1}11)[\bar{1}0\bar{1}]$ slip system. If twinning deformation is an alternative way to accommodate deformation in CdTe, shearing along this direction should be favored because the ratio of slip/twinning Schmid factors is the lowest (0.408). As in the compression experiments, twinning did not occur in the specimen sheared at 1073 K with a load of 40% of CRSS. However, as shown in Fig. 9, three groups of slip bands appeared. One group emerged parallel to the shear direction. This group was probably caused by gliding dislocations driven by shear stress along the $(\bar{1}11)[\bar{1}0\bar{1}]$ slip system. The other two groups originated from gliding dislocations activated along $(\bar{1}11)[\bar{1}0\bar{1}]$ and $(111)[01\bar{1}]$. The $(111)[01\bar{1}]$ is a secondary slip system for the [112] loading axis with a low Schmid factor of 0.272.

To confirm that these slip bands were not twins, x-ray Laue patterns and SEM electron channeling patterns (SEM/ECP) from different specimens or different spots on the same specimen were compared. As shown in Fig. 10(a) and (b), the ECP of an area with dense slip bands was identical to the pattern of an area without slip bands. The twofold symmetry in the patterns is a typical pattern of {110} planes. No pattern variation or pattern rotation could be observed. This confirms that the slip bands are not twins. The ECP observation matches that of the x-ray Laue method, which also did not exhibit a pattern change.

Interestingly, as shown in Table 1, no slip bands could be observed in some of the specimens that were uniaxially compressed along the same direction at a slightly higher temperature and with a heavier load than the shearing experiment. This may be due to a difference in the state of stress. Owing to the arrangement of the shearing device, the specimens were subjected to both normal and shear stresses, whereas the compressed specimens were subjected only to a normal stress. The combination of shear and normal stresses may have caused a higher resolved shear stress on some of the slip systems than that caused by a normal stress alone.

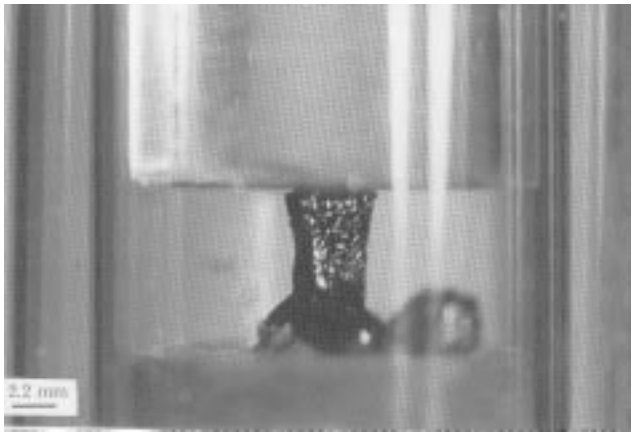

Fig. 8 Plastic deformation of CdTe compressed along [115] at 1353 K for 30 min with 36% CRSS >13.9% strain. The two black chunks are CdTe drops.

3.4 Tensile Deformation

As shown in Fig. 11, the in situ x-ray topograph taken from CdTe tensile stressed in <112> began to distort when the load

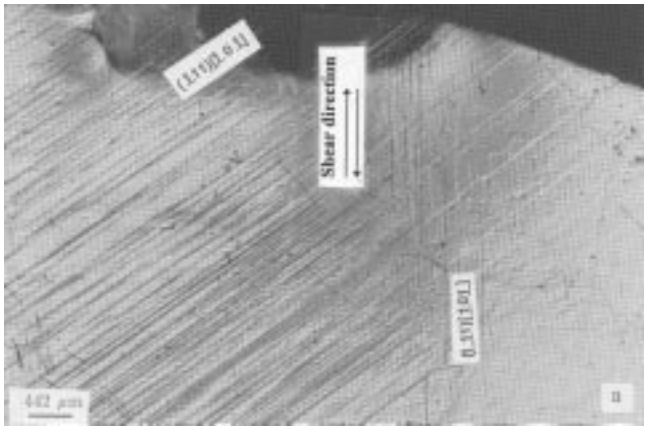

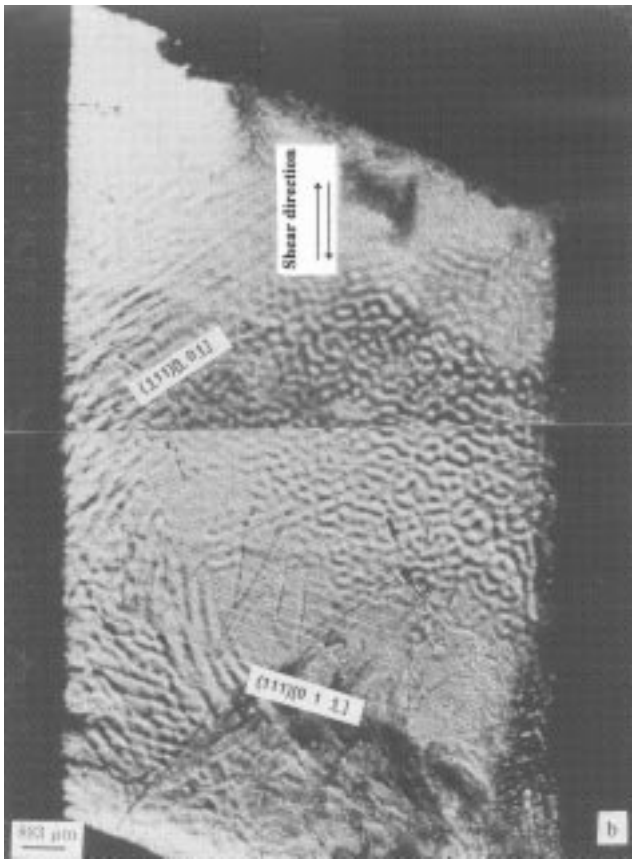

Fig. 9 Three sets of slip bands on the $(\bar{1}10)$ CdTe sheared along $(\bar{1}11)[112]$ at 1073 K for 30 min with 40% CRSS. (a) Slip bands parallel to the shear direction, caused by shear stress. (b) Slip bands caused by compression. The $(111)[01\bar{1}]$ is a secondary slip system for the reference loading axis.

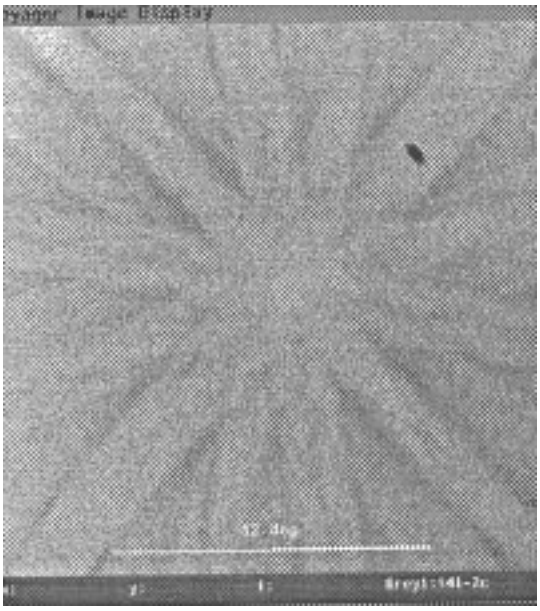

(a)

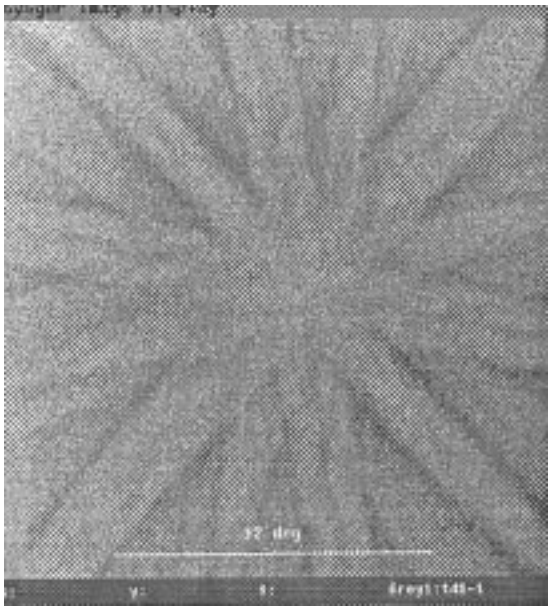

(b)

Fig. 10 Electron channeling patterns from the areas with and without slip bands. The CdTe with the $(\bar{1}10)$ plane was sheared along $(\bar{1}11)[112]$ at 1073 K for 30 min at 40% CRSS. Scanning electron microscope: working voltage, 25 kV; scale length, 12°. (a) The pattern of an area without slip bands. The twofold symmetry is a typical pattern for {110} planes. (b) The pattern of an area with dense slip bands. The pattern of twofold symmetry neither changed nor rotated. The detected area is still a {110} plane.

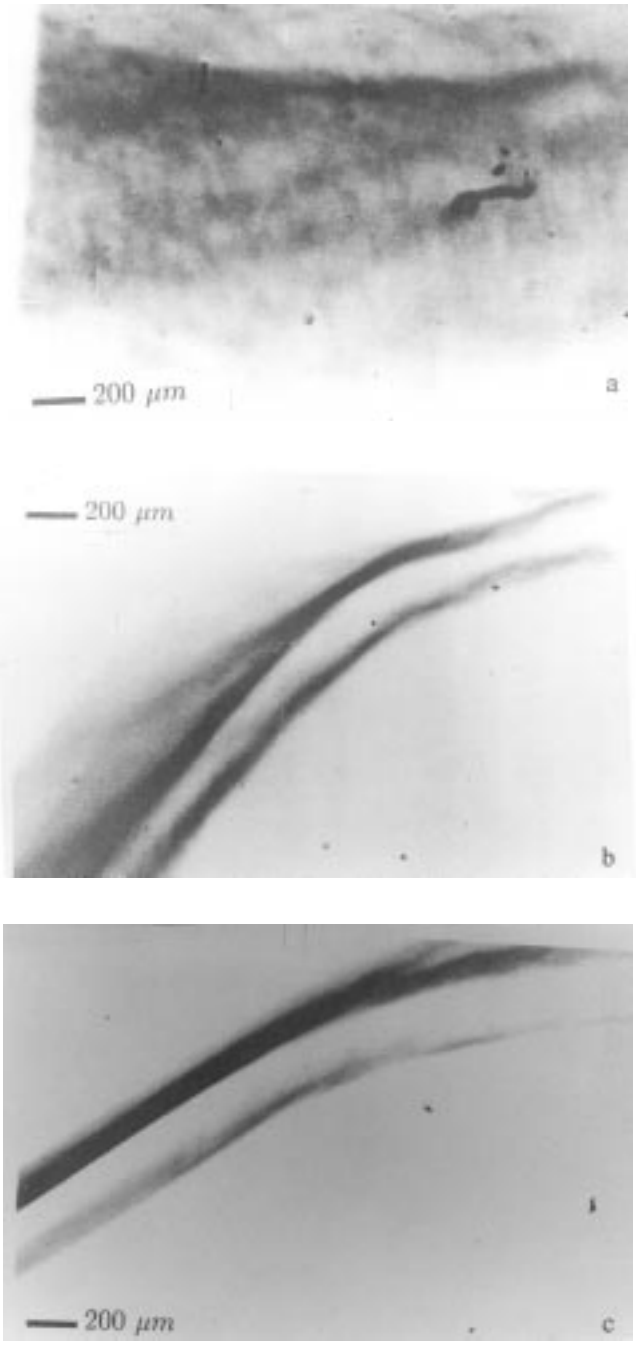

Fig. 11 X-ray topographs of a CdTe tensile specimen at 473 K. (a) At 1.6 MPa, the topograph was not distorted. (b) At 2.0 MPa, the topograph started to distort, indicating lattice rotation caused by deformation. (c) At 2.8 MPa, distorted further

reached about 50% of the CRSS at 473 K. Topographic distortion is caused by rotation of the crystal lattice due to deformation. If twinning had occurred, contrast difference in the form of a twin morphology would have been observed on the topograph. No such feature was recorded. No twins were observed in any specimens tensile stressed along <112> at 373 to 673 K.

The tensile experiments could not be conducted at a higher temperature due to the vaporization of Cd and Te from the specimen surfaces. Due to difficulties such as obtaining accurate orientation and sample alignment, which are frequently encountered with in situ observation with x-ray diffraction techniques, a white beam with a continuous wavelength spectrum was used as the x-ray source. Compared with monochromic x-ray diffraction, a white beam provides poorer resolution in a topograph (Ref 21). In addition to the shortcomings of

white beam diffraction, the fact that CdTe is highly x-ray absorbing made it impossible to conduct tensile experiments at a higher temperature and with a heavier load (Ref 21).

4. Summary

CdTe crystals were uniaxially compressed along several crystallographic axes at temperatures from 773 to 1353 K. The applied loads were from 14 to 74% of the critical resolved shear stress (CRSS) measured in the authors' laboratory. The deformed specimens were annealed without applying stress at temperatures from 573 to 1073 K. No new twins were observed after the above operations. Dense slip bands were observed on most of the compressed specimens. Secondary slip systems were activated in some compression experiments.

CdTe specimens were sheared along {111}<112> at 1073 K with a load of 40% of CRSS. No twins were observed. Three groups of slip bands were observed on the surfaces. One of these was from dislocations gliding on a secondary slip system.

Synchrotron x-ray topography was used to study in situ the effect of stress on crystal deformation. CdTe specimens were uniaxially stressed in tension along <112> at 373 to 673 K. When the load reached about 50% of the CRSS at 473 K, the topograph began to distort, indicating lattice rotation. No twins were observed on the stressed specimens.

Based on the results of compression, shear, and tensile deformation experiments at temperatures ranging from 298 (Ref 1) to 1353 K, it appears that thermal and mechanical stresses in CdTe are released primarily by dislocations gliding on slip systems. Consequently, twinning deformation appears unlikely to occur during CdTe growth. The multiple slip systems, the extremely low CRSS, and weak atomic bonding are so preferential to dislocation motion that massive dislocation glide occurs significantly before twinning deformation. Twins most likely are induced during crystal growth by processes at the growth interface, perhaps involving impurities, supercooling, or stress.

Acknowledgment

This work was supported by the Consortium for Commercial Crystal Growth, one of NASA's Centers for the Commercial Development of Space. The materials used for the experiments were provided by II-VI, Inc., Saxonburg, PA. The Brookhaven National Laboratory and National Institute of Standards and Technology are gratefully acknowledged for allowing the use of the National Synchrotron Light Source.

References

1. A.W. Vere, S. Cole, and D.J. Williams, Twinning in Cadmium Telluride, *J. Electron. Mater.*, Vol 12, 1983, p 551
2. G.R. Awan, A.W. Brinkman, G.J. Russell, and J. Woods, *J. Cryst. Growth*, Vol 85, 1987, p 477
3. P.D. Brown, J.E. Hails, G.L. Russell, and J. Woods, Growth of CdTe Crystals, *J. Cryst. Growth*, Vol 86, 1988, p 511
4. K. Durose and G.J. Russell, Twinning in CdTe, *J. Cryst. Growth*, Vol 101, 1990, p 246
5. T.P. Chen, F.R. Chen, Y.C. Chuang, Y.D. Guo, J.G. Peng, T.S. Huang, and L.J. Chen, Study of Twins in GaAs, GaP and InAs Crystal, *J. Cryst. Growth*, Vol 118, 1992, p 109
6. M. Inoue, I. Teramoto, and S. Takayanagi, *J. Appl. Phys.*, Vol 33, 1962, p 2578
7. H. Iwanaga, N. Shibata, A. Yanaka, and Y. Masa, *J. Cryst. Growth*, Vol 84, 1987, p 345
8. M. Kawano, N. Oda, and T. Sasaki, Twin-Formation Mechanisms for HgCdTe Epilayers, *J. Cryst. Growth*, Vol 117, 1992, p 171
9. G. Dieter, *Mechanical Metallurgy*, 3rd ed., McGraw-Hill Book Company, New York, 1986, p 131-134
10. M.A. Meyers and L.E. Murr, A Model for the Formation of Annealing Twins in F.C.C. Metals and Alloys, *Metallurgica*, Vol 26, 1978, p 951
11. R.L. Fullman and J.C. Fisher, Formation of Annealing Twins during Grain Growth, *J. Appl. Phys.*, Vol 22, 1951, p 1350
12. A.T. Churchman, G.A. Geach, and J. Winton, Deformation Twinning in Materials of the A4 Crystal Structure, *Proc. Roy. Soc. A*, Vol 238, 1956, p 194
13. S. McDevitt, B.E. Dean, D.G. Ryding, F.J. Scheltens, and S. Mahajan, Characterization of CdTe and CdZnTe Single-Crystal Substrates, *Mater. Lett.*, Vol 4, 1986, p 451
14. Y.-C. Lu, Ph.D. dissertation, Stanford University, 1988, p 68
15. I.V. Kurilo and V.I. Kuchma, Twinning in CdTe and CdHgTe Crystals, *Inorg. Mater.*, Vol 18, 1982, p 479
16. E.L Hall and J.B. Van der Sande, On the Nature of Extended Dislocation in Deformed CdTe, *Philos. Mag.*, Vol 37A, 1978, p 137
17. R. Balasubramanian and W.R. Wilcox, Deformation of CdTe at Elevated Temperature, *Mater. Sci. Eng.*, Vol B16, 1993, p 1
18. C. Parfeniuk, F. Weinberg, I.V. Samarasekera, C. Schvezov, and L. Li, *J. Cryst. Growth*, Vol 119, 1992, p 261
19. A. Orlova and B. Sieber, Dislocations in CdTe Plastically Deformed at Room Temperature, *Acta Metall.*, Vol 32, 1984, p 1045
20. J. Shen, D.K. Aidun, L.L. Regel, and W.R. Wilcox, Effect of Annealing on CdTe Microstructure, *Mater. Sci. Eng.*, Vol B16, 1993, p 182
21. R. Balasubramanian, Ph.D. dissertation, Clarkson University, 1992, p 48, 76-77, 112